Cholesterol accumulation in human cornea: evidence that extracellular cholesteryl ester-rich lipid particles deposit independently of foam cells

Paulette M. Gaynor, Wei-Yang Zhang, Bijan Salehizadeh, Brian Pettiford, and Howard S. Kruth[1]

Section of Experimental Atherosclerosis, National Heart, Lung, and Blood Institute, National Institutes of Health, Bethesda, MD 20892

Abstract The cornea is a connective tissue site where lipid accumulates as a peripheral arcus lipoides. We found that cholesterol, in predominantly esterified form, progressively accumulated with age in the peripheral corneas of 20- to 90-yr-old individuals. Ultrastructural studies showed extracellular solid spherical lipid particles (<200 nm in diameter) enmeshed between collagen fibers. Immunostaining showed significant apoE and apoA-I, but very little apoB in the peripheral cornea. Lipid particles were extracted from minced corneas into a buffer and subjected to isopycnic density gradient centrifugation. The lipid particles had a density <1.02 g/ml, contained >75% of their cholesterol in esterified form, and were distributed in two populations with average diameters of 22 ± 5 nm (SD) and 79 ± 26 nm. Gel-filtration chromatographic analysis of the corneal lipid particles showed that most cholesterol eluted with the larger particles and these larger particles lacked apoB. ApoA-I was associated with lipid particles the size of HDL. Most apoE was associated with lipid particles larger than the apoA-I-containing lipid particles and smaller than the large lipid particles that carried most of the corneal cholesterol. Thus, the cholesteryl ester-rich lipid particles that accumulate in the cornea are *1)* similar to lipid particles previously localized within and isolated from human atherosclerotic lesions, *2)* accumulate without foam cells, and *3)* may be derived from low density lipoproteins that have lost their apoB and fused.—**Gaynor, P. M., W-Y. Zhang, B. Salehizadeh, B. Pettiford, and H. S. Kruth.** Cholesterol accumulation in human cornea: evidence that extracellular cholesteryl ester-rich lipid particles deposit independently of foam cells. *J. Lipid Res.* 1996. **37:** 1849–1861.

Supplementary key words atherosclerosis • lipoproteins • apoE • apoA-I • apoB • corneal arcus

The peripheral cornea is a unique site where lipid including cholesterol accumulates (1). Sufficient accumulation of lipid in the peripheral cornea results in a visible circular opacity called arcus lipoides or simply arcus (**Fig. 1**). Deposition of lipid in the peripheral cornea does not interfere with vision. However, there has been interest in the process that results in arcus because of its relevance to the deposition of cholesterol in blood vessels and development of atherosclerotic lesions. The cornea and blood vessels are similar in that both are composed of dense connective tissue (predominantly collagen and glycosaminoglycans) with embedded cells, keratocytes, and smooth muscle cells, respectively (2, 3). Cholesterol deposition in the peripheral cornea and vessel wall are also similar in that deposition is accelerated in both tissues by elevated levels of atherogenic lipoproteins such as low density lipoproteins (LDL) (4, 5). Before the age of 50, the appearance of arcus correlates (independently of plasma cholesterol levels) with premature development of cardiovascular disease (6). In addition, genetic deficiencies of apolipoprotein (apo) A-I and high density lipoproteins (HDL) (considered anti-atherogenic factors) can result in premature development of arcus and atherosclerosis (7–11). Arcus and atherosclerotic coronary artery disease increase with age and the incidence of both is greater in males than in females (12).

One major difference between cholesterol deposition in the cornea and atherosclerotic lesions is that cholesterol deposition in atherosclerotic lesions is accompanied by an infiltration of macrophages (13, 14). These macrophages secrete substances (e.g., cytokines, proteases, complement factors, coagulation factors) that may influence the development of lesions (15). In addition, these macrophages accumulate and store choles-

Abbreviations: LDL, low density lipoproteins; apo, apolipoprotein; HDL, high density lipoproteins; DPBS, Dulbecco's phosphate-buffered saline; BSA, bovine serum albumin; VLDL, very low density lipoproteins; ELISA, enzyme-linked immunosorbent assay; PBS, phosphate-buffered saline; SD, standard deviation; d, density; n, number of particles.

[1]To whom correspondence should be addressed.

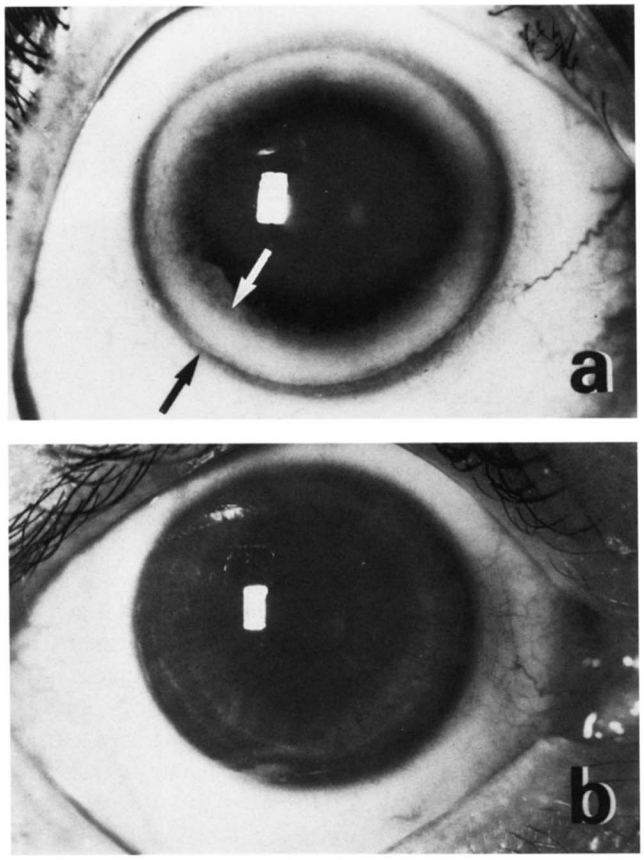

Fig. 1. Photographs comparing eyes with and without peripheral arcus lipoides. Eye of a 75-year-old male with prominent peripheral arcus lipoides (a) and eye of a 44-year-old male without peripheral arcus (b). The paracentral rectangle is an artifact due to reflected light.

terol in lipid droplets that transform the macrophages into so-called foam cells (16). Many investigators consider that the pool of extracellular lipid (which eventually forms the lipid core of atherosclerotic lesions) comes mostly from cholesteryl ester-rich lipid droplets released from dying macrophages. Other investigators believe that this extracellular lipid is derived directly from deposition of atherogenic lipoproteins such as LDL in the extracellular space (17–20).

Evidence for the direct lipoprotein origin of extracellular lipid in lesions is that the size of extracellular lipid particles (<400 nm) is smaller than that of intracellular lipid droplets (>400 nm) (17–19, 21). Also, the fatty acid profile of cholesteryl esters that make up extracellular lipid resembles the profile of plasma lipoproteins (enriched in linoleate) rather than the profile of intracellular lipid droplets (enriched in oleate) (17, 19, 22). However, the possibility remains that extracellular lipid particles are derived from released lipid droplets that become smaller and change their fatty acid composition once these lipid droplets enter the extracellular space. Determining the origin of extracellular lipid in lesions is important because progressive expansion of this lipid pool eventually results in atherosclerotic plaque rupture, thrombosis, and myocardial infarction (18).

Because lipid accumulation in the peripheral cornea may reflect some initial processes of cholesterol deposition that occur in blood vessels, we have examined a number of aspects of the corneal lipid deposition process. First, we have determined the effect of age on the accumulation of the major lipid constituents of lipoproteins (unesterified cholesterol, cholesteryl ester, and phospholipid) in the cornea. Second, we have determined what apolipoproteins are associated with the lipid deposition process in the cornea. Third, we have isolated the lipid particles that accumulate in the cornea. The results of these studies show that cholesteryl ester-rich spherical particles accumulate in the extracellular spaces of the peripheral cornea. Most of these lipid particles are 40–200 nm in diameter and are thus, similar in size to one type of cholesteryl ester-rich lipid particle that accumulates in the extracellular spaces of human atherosclerotic lesions (18, 19, 21). There is controversy about the origin of this extracellular lipid particle as to whether it originates from plasma lipoproteins or intracellular lipid droplets. As the cornea lacks foam cells (14), these extracellular lipid particles cannot be derived from release of lipid droplets from dying foam cells. Rather, these lipid particles appear to be derived from direct deposition and modification of atherogenic plasma lipoproteins.

MATERIALS AND METHODS

Lipid analysis of corneal tissue

Eyes were collected at autopsy within 12 h of death and frozen at -70°C within 4 h of collection. Most corneas were examined for the presence of arcus by slit lamp examination before being frozen. In some cases a corneal–scleral button was prepared from the globe before freezing. For lipid analysis, corneal tissues were thawed, and a corneal–scleral button was cut out from the globes if this had not already been done. Then any remaining sclera was cut away. A 5-mm cork bore was used to punch out the central portion of the cornea. The peripheral and central portions of each cornea were blotted dry and separately weighed. Each portion of cornea was finely minced in 1 ml of dH_2O to pieces no larger than 1 mm^3. Then, each portion was extracted with a mixture of 14 ml of chloroform and 7 ml of methanol as described by Folch, Lees, and Sloane Stanley (23). Unesterified and esterified cholesterol contents were determined enzymatically with the fluorometric method of Gamble et al. (24). Phospholipid content was determined by the method of Bartlett (25).

Immunostaining of apolipoproteins in the cornea

Frozen sections of corneal tissue were prepared. Sections were adhered to gelatin-coated microscope slides and stored at -70°C until immunostaining was carried out. For staining, tissue sections were brought to room temperature and fixed in 10% phosphate-buffered (pH 7.4) formalin for 10 min. All subsequent steps were carried out at room temperature. First, any endogenous peroxidase activity was quenched by treating tissue sections with 3% H_2O_2 for 5 min and two successive rinses in Dulbecco's phosphate-buffered saline (DPBS). Excess buffer was removed from around the sections that were then incubated 15 min with a blocking solution (1% bovine serum albumin [BSA] and 0.1% Tween 20 in DPBS). After the blocking step, sections were incubated with the indicated amounts (in DPBS) of mouse monoclonal primary antibodies. Mouse monoclonal antibodies used were the following: specificity for apoA-I (clone 3F10) and specificity for apoB (clone 2B1) from PerImmune, Inc. (Rockville, MD); and whole ascites fluid with specificity for apoE (MAB 1048) from Chemicon International, Inc. (Temecula, CA). Additionally, a negative staining reaction was assessed by substituting the primary mouse monoclonal antibody with purified mouse IgG (#55939, Cappel, Westchester, PA), or substituting anti-apoE-containing ascites fluid with a similar dilution of control ascites fluid containing an anti-theophylline antibody (#MAB550-215112, Chemicon).

After exposure to primary antibody for 30 min, sections were rinsed twice in DPBS. Detection of the primary antibody was carried out with a kit (LSAB Kit #683, Dako Corp., Carpinteria, CA) that utilized biotin–streptavidin methodology (26). Then, sections were incubated 30 min with biotinylated goat anti-mouse immunoglobulin diluted in DPBS containing 1% BSA and 0.1% Tween 20. After incubation, sections were rinsed twice with DPBS, incubated 30 min with peroxidase-conjugated streptavidin in DPBS, and rinsed twice again with DPBS. Sections were then incubated 10 min with substrate solution consisting of 0.07% 3-amino-9-ethylcarbazole and 0.007% H_2O_2 in 0.1 M acetate buffer (pH 4.8). After a final two rinses, sections were mounted in glycerol–gelatin (#GG-1, Sigma, St. Louis, MO).

Isolation of corneal lipid particles

For isolation of lipid particles, a corneal–scleral button was prepared from globes obtained at autopsy. These specimens were placed into Optisol-GS (Chiron Vision Corp., Irvine, CA) and stored at 4°C for up to 7 days until a sufficient number of corneas could be obtained for analysis. Optisol-GS has been shown to maintain corneas viable for up to 14 days and suitable for transplantation (27). All subsequent procedures were carried out at 4°C. Corneal tissues were removed from Optisol-GS and rinsed at least 2× with buffer containing 50 mM HEPES (pH 7.4), 150 mM NaCl, 2 mM Na_2-EDTA, 0.02% NaN_3, 20 μg/ml aprotinin, 10 μg/ml elastatinal, 1 mM pefabloc SC, 10 μg/ml leupeptin, 2 mM benzamidine, 1 μM D-phe-pro-arg chloromethyl ketone dihydrochloride, 10 μM butylated hydroxytoluene, and 1 μg/ml pepstatin A (buffer A). Then, central and peripheral portions of each cornea were prepared as described above for lipid analysis of corneal tissue. Next, each portion of cornea was minced in 1 ml of buffer A and extracted overnight into buffer A (2 ml total volume). These buffer-extracted lipid particle samples were centrifuged at 500 *g* for 10 min and the resulting supernatant was passed through a filter with 0.45-μm pores (Acrodisc 4184, Gelman Sciences, Ann Arbor, MI).

In some experiments, corneas were frozen within 19 h of death. The corneas were later thawed and lipid particles were isolated as described above. In other experiments, the frozen corneas were thawed, minced, and digested with collagenase (5000 U/g tissue) (Worthington Biochemical Corporation, Freehold, NJ) and soybean trypsin inhibitor (1 mg/ml) (Worthington Biochemical Corporation, Freehold, NJ) in DPBS for 5 h at 37°C before buffer extraction of lipid particles was carried out.

Density gradient fractionation of corneal lipid particles

Samples of buffer-extracted lipid particles were adjusted to d 1.21 g/ml with solid KBr. A discontinuous NaCl gradient was constructed in a 14 × 89-mm ultracentrifuge tube (Ultra-Clear, Beckman Instruments, Palo Alto, CA) from bottom to top with 2 ml of d 1.21 g/ml sample, then 2 ml of d 1.21 g/ml solution without sample, 3 ml of d 1.063 g/ml NaCl solution, 3 ml of d 1.019 g/ml NaCl solution, and 2 ml of d 1.006 g/ml NaCl solution. All density solutions contained 2 mM Na_2-EDTA, pH 7.4, and also the other components (except HEPES) present in buffer A. The gradient was centrifuged (model L5-65 ultracentrifuge, Beckman) in a SW-41 rotor (at 4°C) for 72 h and 200,000 *g*. During centrifugation a continuous gradient was formed as described by Redgrave, Roberts, and West (28). After density gradient centrifugation, the top two 0.8-ml fractions were collected with a small-bore glass pipette (29). The remaining thirteen 0.8-ml fractions were collected with pump-driven aspiration (Auto Densi-Flow II, Haake Buchler, Saddle Brook, NJ) from the top of the gradient.

The refractive indices of the fractions were determined with an Abbe Refractometer (Reichert Co., Buffalo, NY). Corresponding densities were determined by comparison to refractive indices obtained with a control gradient for which densities had been determined with a DMA48 densitometer (Anton Paar, Richmond, VA).

Fractions were analyzed for lipid and apolipoprotein contents. Before analysis of apolipoproteins, gradient fractions were dialyzed against a solution containing 150 mM NaCl, 2 mM Na_2-EDTA, and 0.02% NaN_3 at pH 7.4 (buffer B). Recoveries of cholesterol and apolipoproteins from the density gradient were 88% and >78%, respectively.

Gel-filtration analysis of corneal lipid particles and standards

Three ml of buffer-extracted lipid particles was placed onto a 1.6 × 79-cm, Bio-Gel A-15m (4% agarose) gel-filtration column (Bio-Rad) and eluted with buffer B. Sixty 3-ml fractions were collected at a flow rate of 3.5 ml/h per cm^2. Fractions were analyzed for lipid and apolipoprotein contents. Recoveries of cholesterol and apolipoproteins from the column were 92% and >70%, respectively.

Standards consisted of lipoproteins (HDL [d 1.063–1.21 g/ml], LDL [d 1.019–1.063 g/ml], and very low density lipoproteins [VLDL] [d < 1.006 g/ml]) and apoA-I prepared from human plasma. All were obtained from PerImmune, Inc. Lipoproteins were diluted to 1 mg/ml in buffer B prior to gel-filtration of 1 ml of the lipoprotein sample. ApoA-I was reconstituted into 5 M guanidine HCl at 1 mg/ml (30), dialyzed into buffer B, and passed through a filter with 0.45-μm pores prior to gel-filtration of 1 ml of the apoA-I solution.

Immunoblot analysis of apolipoproteins of corneal lipid particles

Density gradient fractions of buffer-extracted lipid particles were delipidated and concentrated by precipitation with chloroform–methanol according to the procedure of Wessel and Flügge (31). Precipitates were dissolved in a treatment buffer (62.5 mM Tris-HCl [pH 6.8], 10% glycerol, 5% sodium dodecyl sulfate, 2.5% dithiothreitol, and 0.01% Bromophenol Blue) and electrophoresed according to Laemmli (32). Electrophoresis was carried out with 7.5 cm × 10 cm, 10% acrylamide gels and a Mini-Protean II cell (Bio-Rad, Hercules, CA). A Mini Trans-Blot electrophoretic transfer cell (Bio-Rad) was used to blot electrophoresed samples onto nylon membranes. Blotting was carried out in 10 mM 3-(cyclohexylamino)-propanesulfonic acid buffer (pH 9.5) containing 20% methanol. Blots were probed overnight at 4°C with goat polyclonal anti-human apoA-I (2 μg/ml) or apoE (2 μg/ml) antibodies (IgG fraction) (#06500154 and #06501904, Biogenesis). In addition, other blots were probed overnight at 4°C with 1 μg/ml of mouse monoclonal antibodies (purified IgG), clones 6C5, 1D7, and 3H1 (University of Ottawa Heart Institute, Ottawa, Canada), that detect epitopes in the N-terminal, central, and C-terminal regions of the apoE protein, respectively (33). For apoB, the blot was probed overnight at 4°C with 1 μg/ml of goat polyclonal anti-human apoB antibody (IgG fraction from PerImmune, Inc.). Blots were then probed with secondary antibodies, 0.04 μg/ml of affinity-purified, alkaline phosphate-conjugated, rabbit anti-goat or rabbit anti-mouse IgG (Jackson ImmunoResearch Laboratories, Westgrove, PA). Detection was carried out with Lumigen PPD (4-methoxy-4-[3-phosphatephenyl]-spiro[1,2-dioxetane-3,2′-adamantane]) chemiluminescent substrate sheets (Schleicher and Schuell, Keene, NH). Purified apoA-I, apoE, and apoB standards prepared from human plasma were obtained from PerImmune, Inc.

ELISA analysis of apolipoproteins

ApoA-I, apoB, and apoE were quantified using a sandwich-type ELISA. Wells of microtiter plates (96-well Immulon 1, Dynatech, Chantilly, VA) were coated overnight at 4°C with a monoclonal capture antibody in 100 μl of 0.1 M sodium carbonate-bicarbonate buffer, pH 9.6. The monoclonal capture antibody used for apoA-I was clone 3F10 at 5 μg/ml, for apoB was clone 2B4 at 10 μg/ml (PerImmune), and for apoE was clone 6C5 at 1 μg/ml.

After removal of the coating buffer, wells for apoA-I and apoE assays were blocked for 2 h at room temperature with phosphate-buffered saline (PBS) (pH 7.4) containing 2% BSA and 5% sucrose or 3% BSA (PBS-A), respectively. Then, the wells were rinsed 4× with PBS (pH 7.4) containing 0.05% Tween 20 (PBS-T). One hundred-μl samples and apolipoprotein standards were added to wells that were then incubated 2 h for apoA-I and 1 h for apoE at 37°C. Next, wells were rinsed 4× with PBS-T and incubated at 37°C for 1 h with 100 μl of goat polyclonal anti-human apoA-I (2.1 μg/ml) or apoE (3.3 μg/ml) antibodies (#06500154 and 06501904, IgG fractions, Biogenesis Inc., Sandown, NH) diluted in PBS-A. Then, wells were rinsed 4× with PBS-T and incubated at 37°C for 1 h with 100 μl of affinity-purified rabbit polyclonal anti-goat IgG peroxidase conjugate (#A4176, 30 U, Sigma Chemical Co., St. Louis, MO), diluted 1:10,000 into PBS-A. Wells were next rinsed 6× with PBS-T and then incubated 15 min at room temperature with 100 μl of 0.4 g/l 3,3′,5,5′-tetramethylbenzidine (TMB) peroxidase substrate system (#507600, Kirkegaard and Perry Laboratories, Inc., Gaithersburg, MD). Lastly, 100 μl of 2 M sulfonic acid was added to each well and the absorbance at 450 nm was determined.

For the assay of apoB, after removal of the coating buffer, wells were blocked for 1 h at room temperature as described above for apoA-I. One hundred-μl samples and LDL standards were added to wells and incubated 90 min at 37°C. Then, wells were rinsed 6× with PBS-T and incubated at 37°C for 1 h with 100 μl of sheep

polyclonal anti-human apoB peroxidase conjugate (2 μg/ml) (#K90086P, Biodesign, Kennebunk, ME) diluted in PBS (pH 7.4) containing 5% dry milk and 10% normal sheep serum. Next, wells were rinsed 6× with PBS-T and developed with the TMB peroxidase substrate system listed above. Lastly, 1 M sulfonic acid was added and absorbance at 450 nm was determined.

Ultrastructural analysis of cornea and isolated lipid particles

Pieces of cornea (1 mm^3) were prepared for electron microscopic analysis without and with mordanting chemicals to preserve neutral lipid as described by Guyton and Klemp (34). Tissue from peripheral and central regions of corneas from similar aged individuals with and without arcus were examined. Samples of lipid particles isolated from corneas and subjected to density gradient centrifugation were negatively stained and examined by electron microscopy as previously described (35). The dimensions of the isolated lipid particles and those visualized in situ were determined from photomicrographs using digital calipers.

Statistical analysis

Linear regression was used to analyze whether there were significant relationships between age (the independent variable) and the dependent variables that describe the lipid composition of the cornea. Significant differences between the means of the dependent variables describing lipid composition for the central and peripheral cornea were determined using the unpaired Student's *t*-test. A *P*-value ≤0.05 was considered significant for all statistical analyses.

RESULTS

Cholesterol and phospholipid content of corneas

We determined the cholesterol and phospholipid content of the central and peripheral portions of corneas obtained from individuals of ages ranging between 20 and 90 years. Of the 25 corneas studied (all from different donors), arcus was present in corneas of 13 donors (all of whom were >45 years of age); arcus was absent in corneas of 9 donors; and the presence or absence of arcus was not determined for the corneas of 3 donors. All lipids were greater in peripheral as compared with central cornea (**Table 1**). Only esterified cholesterol content was correlated ($r = 0.69$, $P < 0.001$) with age, and this correlation was found only for the peripheral cornea (**Fig. 2**). Esterified cholesterol increased in the peripheral cornea 760 nmol/g for each decade. The percentage of cholesterol that was esterified progressively increased with age ($r = 0.82$, $P < 0.001$ for peripheral cornea and $r = 0.51$, $P < 0.01$ for central cornea), reaching a plateau of 50–70% after age 60 (not

TABLE 1. Analysis of lipid levels in cornea

Lipid Measurement	Peripheral Cornea	Central Cornea
	nmol/g wet wt	
Unesterified cholesterol	2197 ± 188	1014 ± 135
Esterified cholesterol	3018 ± 384	1400 ± 243
Total cholesterol	5215 ± 545	2414 ± 363
Phospholipid	3572 ± 236	2322 ± 274

Shown are the mean (± SEM) lipid levels determined for the 25 corneas studied. Lipid levels in the central and peripheral cornea were significantly different ($P \leq 0.05$) from one another for all lipid constituents listed.

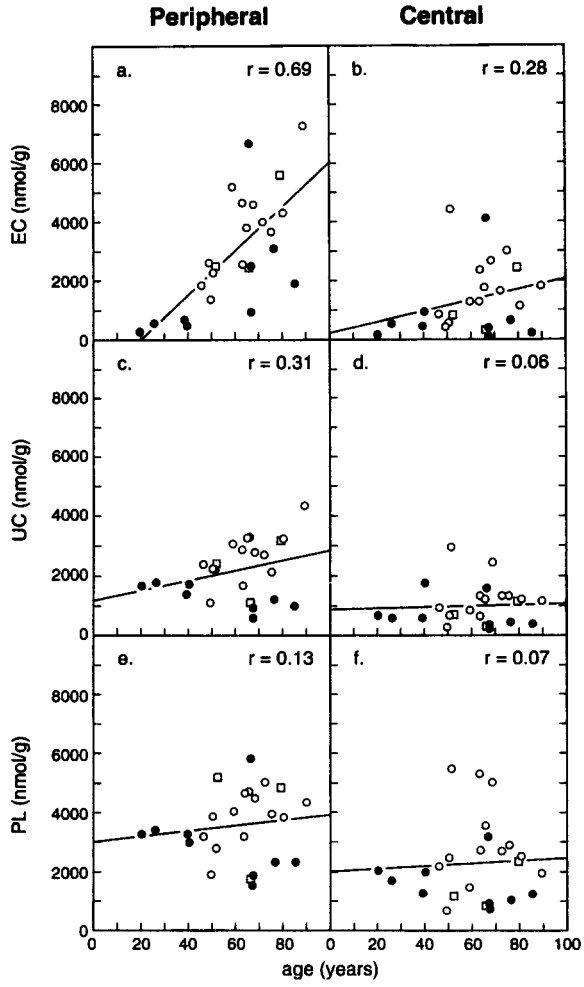

Fig. 2. Effect of age on corneal lipid accumulation. Corneal tissues were dissected into peripheral and central sections (as described under Materials and Methods). Lipids were extracted with chloroform–methanol 2:1 (v/v) and assayed in duplicate for cholesterol and phospholipid. Linear regression analysis of the data was carried out, and correlation coefficients (*r*) (with *P*-values) of age with the dependent variables were calculated; ○, arcus present; ●, arcus absent; □, cornea not examined for arcus; EC, esterified cholesterol; UC, unesterified cholesterol; PL, phospholipid.

shown). Unesterified cholesterol, phospholipid, and the unesterified cholesterol to phospholipid molar ratio showed no correlation with age in either peripheral or central cornea.

Ultrastructural detection of corneal lipid particles

Previous light microscopic studies have shown (with lipid-soluble dyes) that lipid accumulates in the peripheral cornea (14). However, this lipid has not been visualized at the ultrastructural level, because most neutral lipid is extracted during routine preparation of tissue for electron microscopic examination. Special fixation procedures such as those described by Guyton and Klemp (34) are necessary to preserve neutral lipids such as cholesteryl ester. We observed no lipid deposits in the peripheral cornea when this tissue was prepared for electron microscopy using routine procedures (data not shown). When corneal tissue was processed for electron microscopy with a lipid mordanting procedure, single and groups of lipid particles were visualized throughout the extracellular matrix of the peripheral cornea. These lipid particles were solid droplets and only occurred when arcus was present (**Fig. 3**). Most lipid particles ranged in size between 40 and 200 nm in diameter (92 ± 26, average ± SD; number of particles [n] = 417). No lipid droplets were present in cells of corneal tissue, nor were liposomes (i.e., lipid particles with membranes arranged as lamellae) present in the extracellular matrix. Note that lipid particles the size of LDL (≅ 22 nm) are too small to be detected by the method used (34).

Immunostaining of apolipoproteins in cornea

To assess what lipoproteins may be involved in corneal lipid deposition and removal, we evaluated what apolipoproteins were present in the cornea and where they were distributed. Immunostaining of apoA-I and apoE was most intense in the peripheral region of the cornea and was grossly visible in stained sections (**Fig. 4, a and b**). Microscopic examination showed that staining for apoA-I and apoE was panstromal and included Bowman's layer that separates the corneal epithelium and stroma. Most apoA-I and apoE immunostaining occurred in the collagenous matrix of the cornea, but some immunostaining was also associated with the elongated profiles of keratocytes (Fig. 4, insets). It was not possible to distinguish whether the keratocyte-associated staining was located intracellularly or on the plasma membrane surface.

ApoB staining was restricted to the anterior (i.e., front) portion of the peripheral cornea (Fig. 4c) (36) around the region containing the limbal vessels as reported previously (36, 37). ApoB staining was not associated with keratocytes. Replacement of the specific mouse monoclonal antibodies with control antibodies showed no staining of the peripheral or central cornea, and was similar to the lack of staining observed for apoB in the central cornea (Fig. 4c). The pattern of immunostaining for each apolipoprotein was similar for corneas that had arcus and corneas that lacked arcus. However, corneas showed a higher intensity of apoE and apoB immunostaining when arcus was present.

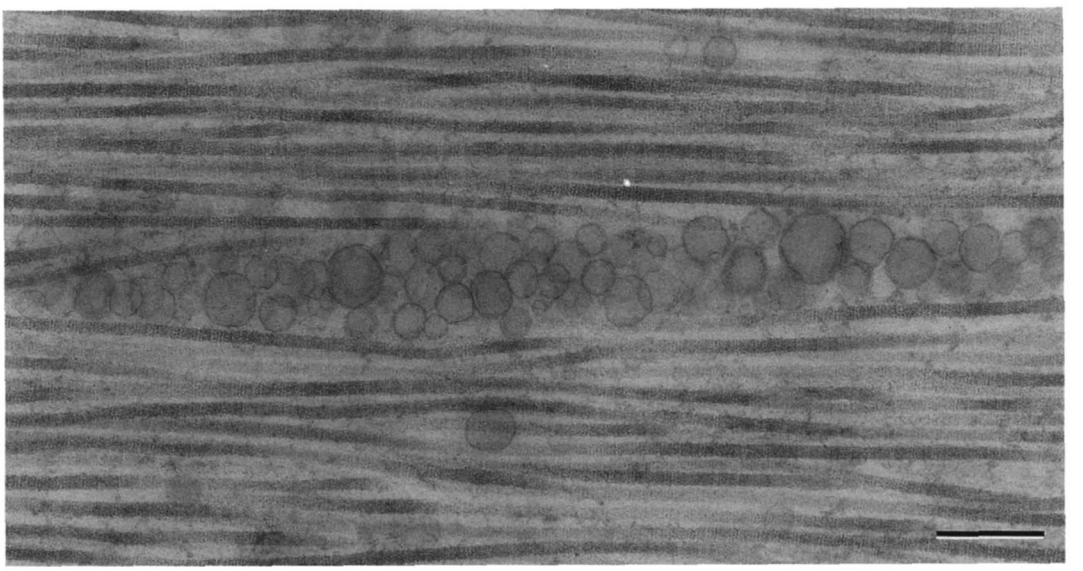

Fig. 3. Ultrastructural detection of lipid particles in the peripheral cornea. A group of spherical particles is shown embedded between the collagen fibers in the extracellular matrix of a cornea that showed arcus. Bar = 200 nm.

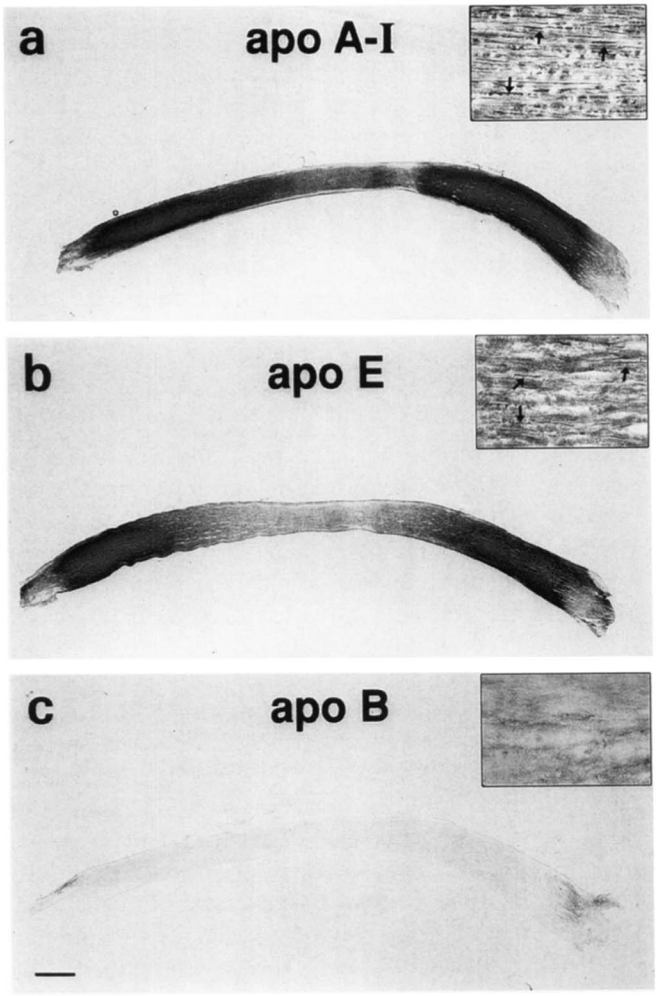

Fig. 4. Immunostaining of apolipoproteins in the human cornea. Frozen cross-sections of a cornea from an individual with arcus were fixed for 10 min with 10% phosphate-buffered formalin. Then, sections were incubated for 30 min with purified (IgG fraction) mouse monoclonal antibodies (1 μg/ml) having specificities for apoA-I or apoB, or with whole mouse ascites fluid (diluted 1:100) containing a monoclonal antibody having specificity for apoE. Control sections were incubated with similar concentrations of purified mouse IgG, or whole ascites fluid containing a monoclonal antibody having specificity for theophylline. Antibodies were detected with a biotin-streptavidin-peroxidase system as described in the Materials and Methods. Incubations with control antibodies showed no staining, similar to the central region of (c). Insets show at higher magnification regions where immunostaining was present. Arrows point to apolipoprotein staining that is associated with linear profiles of keratocytes. Bar = 1 mm for main photomicrographs and 44 μm for insets.

Density gradient fractionation of lipid particles isolated from cornea

Density gradient centrifugation was used to separate buffer-extracted lipid particles from minced central and peripheral corneas with arcus (never frozen). In the peripheral cornea, this procedure resolved one major peak of cholesterol at density (d) < 1.02 g/ml (**Fig. 5a**). Only 2% of cholesterol was contained in fractions with densities similar to that of LDL (1.03–1.05 g/ml). The cholesterol in the d < 1.02 g/ml peak was >75% esterified, and had an unesterified cholesterol to phospholipid molar ratio of 2.1:1. ApoE isolated with cholesteryl ester at d < 1.02, while apoA-I distributed at d > 1.07 g/ml (Fig. 5b and c).

Immunoblot analysis with a polyclonal anti-apoE antibody revealed an apoE doublet around the expected molecular weight of 36 kDa. The doublet bands were consistent with the presence of apoE isoforms showing varying degrees of sialylation (**Fig. 6a**). In addition, apoE bands at higher (67 kDa) and lower (28 kDa and 31 kDa) molecular weights were present. Mouse monoclonal anti-apoE antibodies that detect epitopes near the cen-

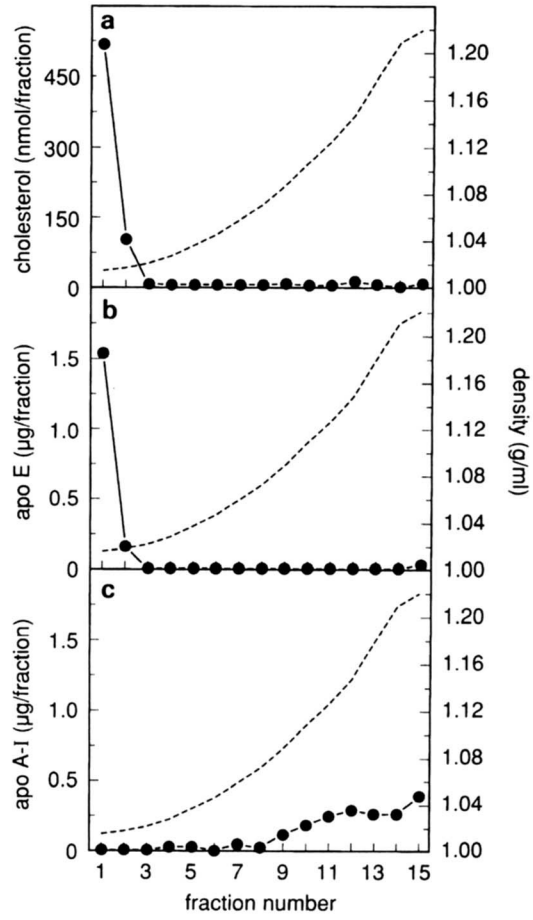

Fig. 5. Density gradient analysis of lipid particles isolated from the peripheral human cornea. Lipid particles were extracted into buffer from corneal tissue (six corneas with arcus from three donors) and then subjected to isopycnic density gradient centrifugation. The buffer-extracted lipid particles were placed at the bottom of the gradient (within the density 1.21 g/ml layer) and centrifuged for 72 h at 200,000 *g*. Fractions were collected and analyzed for cholesterol (a), apoE (b), and apoA-I (c). For ELISA analysis of apolipoproteins, samples were dialyzed into buffer B, and then diluted as needed into buffer B containing 1% BSA for apoE or 1% BSA and 0.05% Tween 20 for apoA-I. ELISA analysis of apoB was not possible because exposure of apoB to the 1.21 g/ml KBr solution irreversibly destroyed apoB immunoreactivity; ●, cholesterol, apoE or apoA-I; - - - -, density.

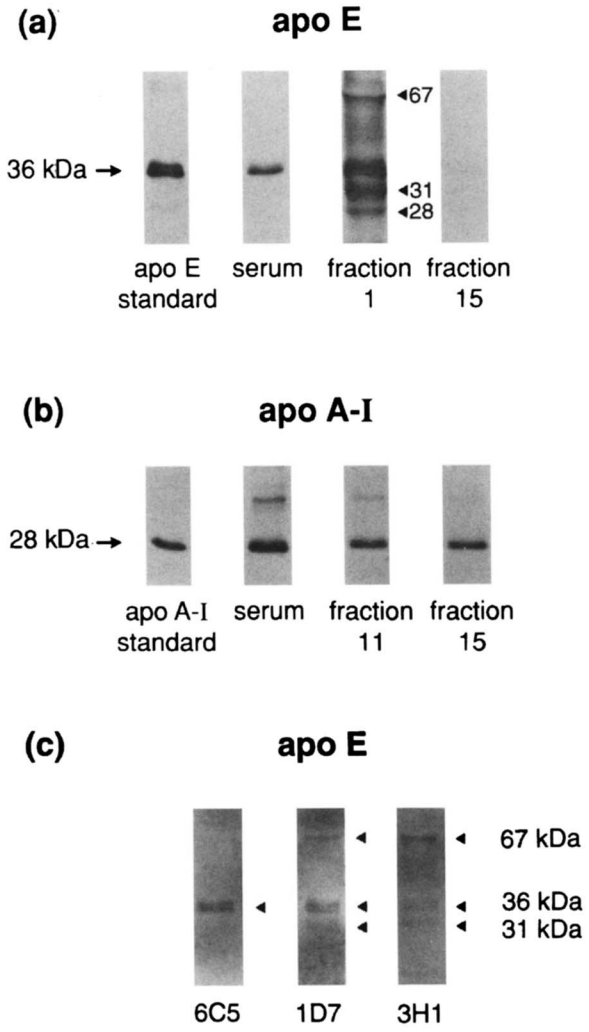

Fig. 6. Immunoblot analysis of apoE and apoA-I protein peaks from density gradient. Samples from the density gradient fractions shown in Fig. 5 were delipidated and concentrated by precipitation with chloroform–methanol. Then, the samples were electrophoresed in 10% acrylamide gels and electroblotted onto nylon membranes. Blots were incubated overnight at 4°C with polyclonal goat IgG antibodies that detected apoE (a) or apoA-I (b) or with monoclonal mouse IgG antibodies that detected epitopes in the N-terminal, central, or C-terminal portions of apoE (6C5, 1D7, 3H1, respectively). The antibodies were detected with chemiluminescence using alkaline phosphatase-conjugated, rabbit anti-goat IgG (a and b) or rabbit anti-mouse IgG (c) and Lumigen PPD as substrate. (a) Fifty ng of apoE (purified from plasma), 1 µl of human serum, 50 µl of fraction 1, and 50 µl of fraction 15 were analyzed; (b) 50 ng of apoA-I (purified from plasma), 1 µl of human serum, 50 µl of fraction 11, and 50 µl of fraction 15 were analyzed; (c) 25 µl of fraction 1 was analyzed in each lane.

tral and in the C-terminal regions of apoE (clones 1D7 and 3H1, respectively) also demonstrated the higher (67 kDa) and one of the lower (31 kDa) molecular weight bands in addition to the doublet at 36 kDa (Fig. 6c). In contrast, clone 6C5 that detects an epitope in the N-terminal region of apoE showed only the doublet at 36 kDa. This showed that this N-terminal epitope was missing from the higher and both lower molecular weight bands. The 67 kDa apoE immunoreactive band was observed under reducing conditions, and thus was not similar to previously identified high molecular weight apoE–protein complexes (38–40).

Immunoblot analysis showed the expected 28 kDa molecular weight for apoA-I in the HDL density fractions and for the lipid-poor apoA-I at densities greater than 1.21 g/ml (Fig. 6b). In data not shown, immunoblot analysis showed apoB only at d 1.03–1.05 g/ml (fractions 4–6). No apoB was detected with the cholesteryl ester-rich lipid particles at d < 1.02 g/ml.

Buffer-extracted lipid particles from the central cornea showed a density gradient distribution of cholesterol and apolipoproteins similar to that of the peripheral cornea. However, the levels of cholesterol, apoA-I, and apoE in the central cornea were lower as compared with the levels of these constituents in the peripheral cornea (cholesterol was 22%, apoE was 14%, and apoA-I was 65% of their respective levels in peripheral cornea).

Negatively stained cholesteryl ester-rich lipid particles at d < 1.02 g/ml were <200 nm in diameter. Two populations of spherical particles were observed. One population was composed of particles similar in size to LDL (**Fig. 7,** inset to the upper panel), and the other population was composed of particles that were larger than LDL (Fig. 7, upper panel). The population of smaller particles had an average diameter of 22 ± 5 (SD) nm (n = 216) similar to LDL, and the population of larger particles had an average diameter of 79 ± 26 nm (n = 630) (Fig. 7, lower panel). In the central cornea the cholesteryl ester-rich lipid particles at d < 1.02 g/ml were also spherical, but showed only one population of particles with an average diameter of 76 ± 13 nm (n = 282).

Density gradient analysis was also carried out for lipid particles released from corneas that had been stored frozen. Particles from these corneas were isolated from buffer extracts of minced corneas or corneas minced and then digested with collagenase. Collagenase digestion released 83% of the lipid contained within the cornea. This was greater than the 52 and 55% released from minced corneas that were not digested with collagenase. The density gradient distributions of cholesterol and apolipoproteins obtained with buffer-extracted lipid particles from minced corneas (with or without collagenase digestion) that had been frozen were similar to the distributions obtained with buffer-extracted lipid particles from minced corneas that had never been frozen (data not shown).

Lastly, density gradient analysis of buffer-extracted lipid particles prepared from four minced corneas with-

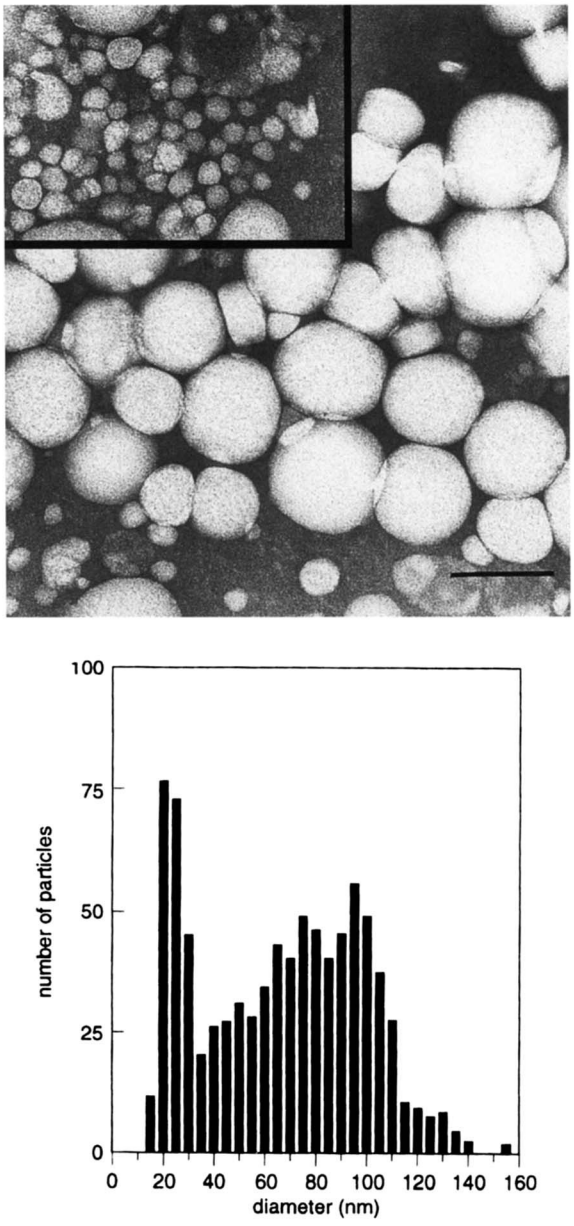

Fig. 7. Ultrastructural analysis and size distribution of the d < 1.02 g/ml fraction of arcus lipid particles. Ten µl of the d < 1.02 g/ml lipid particle fraction isolated from the peripheral cornea was negatively stained with 2% sodium phosphotungstic acid and examined with an electron microscope (upper panel). The diameters of 846 particles were determined from photomicrographs (lower panel). The spherical lipid particles distributed into two populations with an average diameter of 22 ± 5 (SD) nm and 79 ± 26 nm. Inset shows a group of the smaller-sized lipid particles. The bar in the upper panel = 100 nm.

out arcus (from two individuals) showed a distribution of apoA-I similar to the distribution shown in Fig. 5c for corneas with arcus. However, buffer-extracted lipid particles from these corneas without arcus lacked the cholesterol and apoE at d < 1.02 g/ml (data not shown) that corneas with arcus showed.

Analysis of corneal lipid particles by gel-filtration chromatography

Gel-filtration chromatography was carried out to determine how much cholesterol was carried in the LDL-sized particles compared with the larger lipid particles. Buffer-extracted lipid particles from combined minced corneas with and without arcus were analyzed. Most cholesterol in the corneal lipid particles eluted in the column void volume well before the elution position of plasma LDL (**Fig. 8a**). The cholesterol in the void volume (fractions 17–21) was 76% esterified, and had an unesterified cholesterol to phospholipid molar ratio of 1.6:1. The fractions containing apoB (fractions 32–40 shown in Fig. 8c) eluted similar to that of plasma LDL and contained only 4% of the cholesterol that eluted from the column. Very little apoB was observed within the void volume (fractions 17–21) which contained most of the eluted cholesterol.

ApoE from the cornea eluted in fractions that extended from the void volume to the elution position of LDL (Fig. 8b). Only a small amount of apoE co-isolated with the large lipid particles that carried most of the corneal cholesterol (i.e., V_o fractions 17–21). The majority of the apoE eluted with lipid particles smaller (i.e., fractions 22–40) than the large lipid particles. Most apoA-I from the cornea eluted in the general region where purified plasma HDL eluted (Fig. 8d). This finding was consistent with the density gradient profile of apoA-I that in addition showed 37% of apoA-I isolated as lipid-poor apoA-I (d > 1.21 g/ml). The presence of lipid-poor apoA-I could reflect the tendency of apoA-I to dissociate from HDL during high speed ultracentrifugation (41). However, because HDL was not sufficiently separated from purified apoA-I standard by the gel-filtration column used, confirming the presence of lipid-poor apoA-I in the cornea was not possible.

DISCUSSION

Our findings show that extracellular cholesteryl ester-rich lipid particles accumulate in the human cornea. These corneal lipid particles are similar to a type described by Chao et al. (19) that accumulate in human atherosclerotic lesions. Both are about 40 to 200 nm in diameter, cholesteryl ester-rich, low density (d < 1.02 g/ml) spherical droplets that accumulate extracellularly. Because the size of these extracellular lipid particles is greater than that of plasma-derived LDL but less than that of intracellular lipid droplets, the origin of these lipid particles in atherosclerotic lesions has been controversial. As the adult human cornea normally lacks macrophages and foam cells (14), our findings in cornea show that this type of extracellular lipid particle can

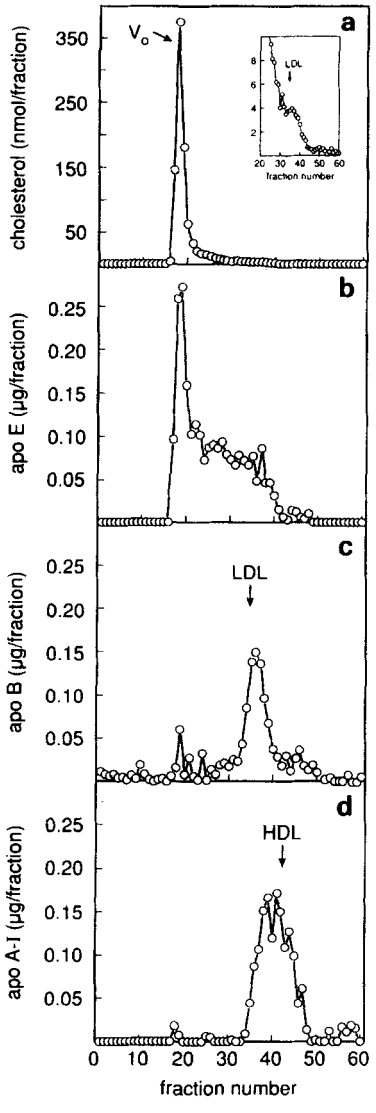

Fig. 8. Gel-filtration chromatographic analysis of isolated corneal lipid particles. Lipid particles were extracted into buffer from corneal tissue (eight corneas [6 with and 2 without arcus] from five donors) and then passed over a 1.6 × 79 cm, 4% agarose gel-filtration column. Sixty 3-ml fractions were collected and analyzed for cholesterol (a), apoE (b), apoB (c), and apoA-I (d). For ELISA analysis of apoA-I, samples were diluted 1:1 with 2% BSA and 1% Tween 20 in a column buffer (i.e., buffer B). For ELISA analysis of apoE and apoB, samples were assayed undiluted. Elution positions of purified plasma LDL and HDL are indicated. VLDL eluted with the void volume. Purified human apoA-I eluted three fractions later than HDL (not shown). V_o, void volume.

accumulate in the absence of release of cholesteryl ester-rich lipid droplets from foam cells.

A second type of extracellular lipid particle found in atherosclerotic lesions, unesterified cholesterol-rich liposomes (19), is absent from the cornea. A relationship between the formation of these liposomes and foam cells is suggested by the observation that foam cells are usually surrounded by the liposomes in the vessel wall (42). Robenek and Schmitz (43) have shown that macrophages can produce unesterified cholesterol-rich liposomes during processing of lipoprotein-derived cholesteryl ester. The fact that liposomes do not occur in the cornea further implicates the macrophage as a factor in the formation of these liposomes.

If extracellular cholesteryl ester-rich lipid droplets are not derived from intracellular lipid droplets, where do they come from? One source of the cholesteryl ester that accumulates in the cornea and also in atherosclerotic lesions is thought to be LDL. This is because the development of arcus in the cornea, similar to the development of atherosclerotic lesions, is accelerated by high plasma levels of LDL (4, 5). Additionally, apoB, the major protein constituent of LDL, is found in the peripheral cornea (36, 37). However, significant amounts of LDL were not detected in a previous investigation that analyzed buffer-extracted lipid particles with electrophoresis (44, 45). Furthermore, the cholesterol in these buffer-extracted lipid particles greatly exceeded the apoB that should have been present if deposited cholesterol was derived solely from LDL. Earlier work from our laboratory showed that lipid extending from the front to the back of the cornea could be detected in advanced arcus. However, apoB was present mostly toward the front of the cornea and could be absent from areas of the cornea (especially toward the back of the cornea) that showed significant lipid staining (36).

The results of the present study show that these earlier findings can be explained by the presence in the cornea of cholesteryl ester-rich lipid droplets that are deficient in apoB. The corneal lipid particles are on average about 4-times larger in diameter and of lower density ($d < 1.02$ g/ml) compared with LDL (LDL are spherical 22-nm particles of d 1.019–1.063 g/ml). All these findings suggest that if LDL is the source of cholesterol that accumulates in the cornea, then this lipoprotein must be significantly modified such that its apoB component is lost and its size and density are altered. Only about 4% and 2% of corneal lipid particle cholesterol were recovered in lipid particles that had a similar size and density, respectively, to LDL. LDL-sized and larger lipid particles of $d < 1.02$ g/ml showed no evidence of apoB by Western blot analysis. ApoB was observed by Western blot analysis only for lipid particles in the peak LDL density range (d 1.03–1.05 g/ml).

The $d < 1.02$ g/ml corneal lipid particles could be derived from LDL that lost apoB, with some of these apoB-deficient LDL particles then fusing to form larger apoB-deficient lipid particles. Proteolysis of apoB is a possible mechanism by which apoB may be lost from LDL and at the same time that can cause fusion of the LDL particles. Kovanen and Kokkonen (20) and Piha,

Lindstedt, and Kovanen (46) have shown that enzymes of mast cells, chymase and tryptase, can degrade apoB sufficiently to cause fusion of LDL particles. Mast cells are normally absent from the cornea but are present at the limbus (47), the same location where plasma-derived lipoproteins enter the cornea from the limbal vasculature (11). Thus, it is conceivable that mast cell enzymes also enter the cornea but this has not been studied.

Further evidence that LDL can convert to larger-sized particles comes from in vivo studies in which LDL was injected into the blood stream of rabbits (48). This procedure induced accumulation by 2 h of what was interpreted to be fused LDL (as large as 161 nm) within the subendothelial region of the aorta. In the human cornea and aorta, apoB immunoreactivity is found in regions closest to the blood supply, while apoB immunoreactivity is less or absent in regions furthest from the blood supply, although lipid accumulates in both regions (36, 49). Thus, complete loss of apoB from deposited lipoprotein particles appears to occur in humans in regions farthest from the blood supply. It is conceivable that tissue regions distant from the blood supply are deficient in blood-derived protease inhibitors.

Studies have suggested a role for chylomicron remnant lipoproteins in the development of atherosclerosis (50). Chylomicron remnants are similar in size (51, 52) to the fraction of large cholesteryl ester-rich lipid particles isolated from corneas. However, it is unlikely that chylomicron remnants are the source of these lipid particles, because the large size of chylomicron remnants should preclude their diffusion through the matrix of the cornea (53). It is more likely that smaller lipoproteins such as LDL diffuse into the cornea, fuse, and then become trapped in this matrix.

Only a small amount of apoE co-isolated with the large corneal lipid particles that carried most of the corneal cholesterol. ApoE is not a usual component of LDL, but is associated with chylomicrons, VLDL, and their remnants. Most apoE in the cornea was associated with cholesteryl ester-rich lipid particles that were smaller than chylomicron remnants and VLDL. VLDL remnants formed during lipolysis of VLDL triglyceride would be expected to be in this size range. Moreover, lipolysis of VLDL triglyceride is associated with degradation of apoB and apoE (54). Degradation is due to an endogenous protease associated with VLDL that results in lower molecular weight fragments (28 kDa and 31 kDa) of apoE identical to what we observed for cornea apoE. We could not detect apoB in the large cholesteryl ester-rich lipid particles by Western blotting, although we did detect apoE. It is possible that not only was apoB degraded in these lipid particles, but that it was oxidized as well. This could interfere with immunodetection of apoB because oxidation impairs immunoreactivity (55). It has been shown that apoB in VLDL is more susceptible than apoE in VLDL to oxidation (56).

The greatest deposit of lipid and apolipoproteins occurred in the peripheral cornea. This may reflect the fact that the peripheral cornea receives the greatest degree of perfusion that comes from the limbal vasculature (57). Also, differences in the structure of the cornea may limit diffusion of lipid particles from the peripheral cornea (where the limbal vasculature is located) to the central cornea (reviewed in ref. 11). Collagen fibrils are more tightly packed in the central as compared with the peripheral cornea. Based on permeability studies, it has been suggested that the largest molecule capable of diffusing across the human cornea would be about 12 nm in diameter (53). Thus, diffusion of particles the size of apoE-containing VLDL remnants into the center of the cornea should be restricted. This could explain the greater apoE immunostaining present in the peripheral as compared with the central cornea.

It is likely that the HDL-like lipoproteins we found in the cornea are derived from the blood and function to remove cholesterol from the cornea (rather than contributing cholesterol to the cornea). Unlike high blood levels of LDL, high levels of HDL are not associated with accelerated development of corneal arcus. Furthermore, disturbances in HDL metabolism due to genetic deficiencies of apoA-I and lecithin:cholesterol acyltransferase (an enzyme that esterifies unesterified cholesterol acquired by HDL) are associated with accelerated development of corneal arcus (7–11).

Generally, the absence of arcus was associated with lower levels of corneal lipid (Fig. 2). However, one cornea from a 66-year-old donor contained the second highest cholesteryl ester content but displayed no arcus. This suggests that other factors besides absolute lipid content of the cornea contribute to the presence or absence of arcus. Larger lipid particles scatter more light than smaller lipid particles. Thus, the relative amounts of large (40–200 nm) and small (LDL-sized, <30 nm) lipid particles that accumulate in the cornea may determine whether the cornea will show an arcus.

We have shown in this study that deposition of extracellular cholesteryl ester can occur independently of foam cells that are absent from the normal human cornea. Thus, extracellular lipid droplets do not need to be derived from release of intracellular lipid droplets. Alternatively, the findings in the cornea suggest that extracellular lipid droplets are derived from direct deposition of plasma lipoproteins. These lipoproteins could be derived from fusion of protein-deficient LDL. Such fused LDL may become trapped in the extracellular matrix due to their size (58) and because protein-deficient LDL show an enhanced affinity for the extracellu-

lar matrix (59). Deposition of extracellular cholesteryl ester highly correlates with the development of atherosclerotic lesions (60). Thus, determining the origin of this lipid is helpful to learning why this lipid accumulates and also how this lipid may accelerate atherosclerosis.

We thank Dr. Sally Hunsberger (Division of Epidemiology and Clinical Applications, NHLBI) for help with statistical analysis; Dr. Wendy Taddei-Peters (PerImmune, Inc.) for suggestions concerning ELISA analysis of apolipoproteins; Ina Ifrim, Rani Rao, and Janet Chang for help in carrying out these experiments; Kim Allen and The Lions Eye Bank of Washington for collecting corneal tissue; Carol Kosh for help in preparing the manuscript; and Dr. David Cogan for providing the photograph of arcus.

Manuscript received 31 January 1996 and in revised form 6 June 1996.

REFERENCES

1. Broekhuyse, R. M. 1975. The lipid composition of aging sclera and cornea. *Ophthalmologica.* **171:** 82–85.
2. Klyce, S. D., and R. W. Beuerman. 1988. Structure and function of the cornea. *In* The Cornea. H. E. Kaufman, M. B. McDonald, B. A. Barron, and S. R. Waltman, editors. Churchill Livingstone, New York, NY. 3–54.
3. Fawcett, D. W., and E. Raviola. 1994. Bloom and Fawcett, a Textbook of Histology. Chapman and Hall, New York, NY. 368–377.
4. Rifkind, B. M., and C. Dickson. 1965. The incidence of arcus senilis in ischaemic heart disease. Its relation to serum-lipid levels. *Lancet.* **1:** 312–314.
5. Rifkind, B. M. 1972. Corneal arcus and hyperlipoproteinaemia. *Surv. Ophthalmol.* **16:** 295–304.
6. Chambless, L. E., F. D. Fuchs, S. Linn, S. B. Kritchevsky, J. C. Larosa, P. Segal, and B. M. Rifkind. 1990. The association of corneal arcus with coronary heart disease and cardiovascular disease mortality in the Lipid Research Clinics mortality follow-up study. *Am. J. Public Health.* **80:** 1200–1204.
7. Winder, A. F., and L. K. Borysiewics. 1982. Corneal opacification and familial disorders affecting plasma high-density lipoprotein. *Birth Defects.* **18:** 433–440.
8. Schaefer, E. J., J. R. McNamara, C. J. Mitri, and J. M. Ordovas. 1986. Genetic high density lipoprotein deficiency states and atherosclerosis. *Adv. Exp. Med. Biol.* **201:** 1–15.
9. Bron, A. J. 1989. Corneal changes in the dislipoproteinaemias. *Cornea.* **8:** 135–140.
10. Barchiesi, B. J., R. H. Eckel, and P. P. Ellis. 1991. The cornea and disorders of lipid metabolism. *Surv. Ophthalmol.* **36:** 1–22.
11. Crispin, S. M. 1989. Lipid deposition at the limbus. *Eye.* **3:** 240–250.
12. Pe'er, J., J. Vidaurri, S-T. Halfon, S. Eisenberg, and H. Zauberman. 1983. Association between corneal arcus and some of the risk factors for coronary artery disease. *Br. J. Ophthalmol.* **67:** 795–798.
13. Gerrity, R. G., H. K. Naito, M. Richardson, and C. J. Schwartz. 1979. Dietary induced atherogenesis in swine. Morphology of the intima in prelesion stages. *Am. J. Pathol.* **95:** 775–792.
14. Cogan, D. G., and T. Kuwabara. 1959. Arcus senilis. Its pathology and histochemistry. *Arch. Ophthalmol.* **61:** 553–560.
15. Nathan, C. F. 1987. Secretory products of macrophage. *J. Clin. Invest.* **79:** 319–326.
16. Gerrity, R. G. 1981. The role of the monocyte in atherogenesis. I. Transition of blood-borne monocytes into foam cells in fatty lesions. *Am. J. Pathol.* **103:** 181–190.
17. Smith, E. B. 1974. The relationship between plasma and tissue lipids in human atherosclerosis. *Adv. Lipid Res.* **12:** 1–49.
18. Guyton, J. R., K. F. Klemp, B. L. Black, and T. M. A. Bocan. 1990. Extracellular lipid deposition in atherosclerosis. *Eur. Heart J.* **(Supp E)11:** 20–28.
19. Chao, F-F., E. J. Blanchette-Mackie, Y-J. Chen, B. F. Dickens, E. Berlin, L. M. Amende, S. I. Skarlatos, W. Gamble, J. H. Resau, W. T. Mergner, and H. S. Kruth. 1990. Characterization of two unique cholesterol-rich lipid particles isolated from human atherosclerotic lesions. *Am. J. Pathol.* **136:** 169–179.
20. Kovanen, P. T., and J. O. Kokkonen. 1991. Modification of low density lipoproteins by secretory granules of rat serosal mast cells. *J. Biol. Chem.* **266:** 4430–4436.
21. Kruth, H. S. 1984. Histochemical detection of esterified cholesterol within human atherosclerotic lesions using the fluorescent probe filipin. *Atherosclerosis.* **51:** 281–292.
22. Guyton, J. R., and K. F. Klemp. 1994. Development of the atherosclerotic core region. Chemical and ultrastructural analysis of microdissected atherosclerotic lesions from human aorta. *Arterioscler. Thromb.* **14:** 1305–1314.
23. Folch, J., M. Lees, and G. H. Sloane Stanley. 1957. A simple method for the isolation and purification of total lipids from animal tissues. *J. Biol. Chem.* **226:** 497–509.
24. Gamble, W., M. Vaughan, H. S. Kruth, and J. Avigan. 1978. Procedure for determination of free and total cholesterol in micro- or nanogram amounts suitable for studies with cultured cells. *J. Lipid Res.* **19:** 1068–1070.
25. Bartlett, G. R. 1959. Phosphorous assay in column chromatography. *J. Biol. Chem.* **234:** 466–468.
26. Guesdon, J-L., T. Ternynck, and S. Avrameas. 1979. The use of avidin-biotin interaction in immunoenzymatic techniques. *J. Histochem. Cytochem.* **27:** 1131–1139.
27. Lindstrom, R. L., H. E. Kaufman, D. L. Skelnik, R. A. Laing, J. H. Lass, D. C. Musch, M. D. Trousdale, W. J. Reinhart, T. E. Burris, A. Sugar, R. M. Davis, K. Hirokawa, T. Smith, and J. F. Gordon. 1992. Optisol corneal storage medium. *Am. J. Ophthalmol.* **114:** 345–356.
28. Redgrave, T. G., D. C. K. Roberts, and C. E. West. 1975. Separation of plasma lipoproteins by density-gradient ultracentrifugation. *Anal. Biochem.* **65:** 42–49.
29. Mills, G. L., P. A. Lane, and P. K. Weech. 1984. A Guidbook to Lipoprotein Technique. Elsevier, New York, NY. 50–54.
30. Jonas, A., and W. R. Mason. 1981. Interactions of dipalmitoyl- and dimyristoylphosphatidylcholines and their mixtures with apolipoprotein A-I. *Biochemistry.* **20:** 3801–3805.
31. Wessel, D., and U. I. Flügge. 1984. A method for the quantitative recovery of protein in dilute solution in the presence of detergents and lipids. *Anal. Biochem.* **138:** 141–143.
32. Laemmli, U. K. 1970. Cleavage of structural proteins during the assembly of the head of bacteriophage T4. *Nature.* **227:** 680–685.

33. Weisgraber, K. H., S. C. Rall, Jr., R. W. Mahley, R. W. Milne, Y. L. Marcel, and J. T. Sparrow. 1986. Human apolipoprotein E. Determination of the heparin binding sites of apolipoprotein E3. *J. Biol. Chem.* **261:** 2068–2076.
34. Guyton, J. R., and K. F. Klemp. 1988. Ultrastructural discrimination of lipid droplets and vesicles in atherosclerosis: value of osmium-thiocarbohydrazide-osmium and tannic acid-paraphenylenediamine techniques. *J. Histochem. Cytochem.* **36:** 1319–1328.
35. Kruth, H. S., S. I. Skarlatos, P. M. Gaynor, and W. Gamble. 1994. Production of cholesterol-enriched nascent high density lipoproteins by human monocyte-derived macrophages is a mechanism that contributes to macrophage cholesterol efflux. *J. Biol. Chem.* **269:** 24511–24518.
36. Ashraf, F., D. G. Cogan, and H. S. Kruth. 1993. Apolipoprotein A-I and B distribution in the human cornea. *Invest. Ophthalmol. Vis. Sci.* **34:** 3574–3578.
37. Walton, K. W. 1973. Studies on the pathogenesis of corneal arcus formation. I. The human corneal arcus and its relation to atherosclerosis as studied by immunofluorescence. *J. Pathol.* **111:** 263–274.
38. Weisgraber, K. H., and R. W. Mahley. 1978. Apoprotein (E-A-II) complex of human plasma lipoproteins. I. Characterization of this mixed disulfide and its identification in a high density lipoprotein subfraction. *J. Biol. Chem.* **253:** 6281–6288.
39. Tozuka, M., H. Hidaka, M. Miyachi, K-I. Furihata, T. Katsuyama, and M. Kanai. 1992. Identification and characterization of apolipoprotein (AII-E2-AII) complex in human plasma lipoprotein. *Biochim. Biophys. Acta.* **1165:** 61–67.
40. Weisgraber, K. H., and L. H. Shinto. 1991. Identification of the disulfide-linked homodimer of apolipoprotein E3 in plasma. Impact on receptor binding activity. *J. Biol. Chem.* **266:** 12029–12034.
41. Kunitake, S. T., and J. P. Kane. 1982. Factors affecting the integrity of high density lipoproteins in the ultracentrifuge. *J. Lipid Res.* **23:** 936–940.
42. Kruth, H. S. 1984. Localization of unesterified cholesterol in human atherosclerotic lesions. Demonstration of filipin-positive, oil red O-negative particles. *Am. J. Pathol.* **114:** 201–208.
43. Robenek, H., and G. Schmitz. 1988. Ca^{++} antagonists and ACAT inhibitors promote cholesterol efflux from macrophages by different mechanisms. II. Characterization of intracellular morphologic changes. *Arteriosclerosis.* **8:** 57–67.
44. Sheraidah, G. A. K., A. F. Winder, and A. R. Fielder. 1981. Lipid-protein constituents of human corneal arcus. *Atherosclerosis.* **40:** 91–98.
45. Winder, A. F., G. Sheraidah, and A. R. Fielder. 1978. Plasma low-density lipoprotein and the composition of human corneal arcus. *Biochem. Soc. Trans.* **6:** 1392–1393.
46. Piha, M., L. Lindstedt, and P. T. Kovanen. 1995. Fusion of proteolyzed low-density lipoprotein in the fluid phase: a novel mechanism generating atherogenic lipoprotein particles. *Biochemistry.* **34:** 10120–10129.
47. Allansmith, M. R., and R. N. Ross. 1988. Ocular allergy. *Clin. Allergy.* **18:** 1–13.
48. Nievelstein, P. F. E. M., A. M. Fogelman, G. Mottino, and J. S. Frank. 1991. Lipid accumulation in rabbit aortic intima 2 hours after bolus infusion of low density lipoprotein. A deep-etch and immunolocalization study of ultrarapidly frozen tissue. *Arterioscler. Thromb.* **11:** 1795–1805.
49. Kruth, H. S., and B. Shekhonin. 1994. Evidence for loss of apoB from LDL in human atherosclerotic lesions: extracellular cholesteryl ester lipid particles lacking apoB. *Atherosclerosis.* **105:** 227–234.
50. Havel, R. J. 1994. Postprandial hyperlipidemia and remnant lipoproteins. *Curr. Opin. Lipidol.* **5:** 102–109.
51. Fainaru, M., R. W. Mahley, R. L. Hamilton, and T. L. Innerarity. 1982. Structural and metabolic heterogeneity of β-very low density lipoproteins from cholesterol-fed dogs and from humans with Type III hyperlipoproteinemia. *J. Lipid Res.* **23:** 702–714.
52. Bersot, T. P., T. L. Innerarity, R. W. Mahley, and R. J. Havel. 1983. Cholesteryl ester accumulation in mouse peritoneal macrophages induced by β-migrating very low density lipoproteins from patients with atypical dysbetalipoproteinemia. *J. Clin. Invest.* **72:** 1024–1033.
53. Maurice, D. M. 1961. The use of permeability studies in the investigation of submicroscopic structure. *In* The Structure of the Eye. G. K. Smelser, editor. Academic Press, New York, NY. 381–391.
54. Chung, B. H., J. H. Im, and H. R. Bowdon. 1986. Lipolysis-induced degradation of apolipoproteins B and E of human very low density lipoproteins. *J. Biol. Chem.* **261:** 2960–2967.
55. Zawadzki, Z., R. W. Milne, and Y. L. Marcel. 1989. An immunochemical marker of low density lipoprotein oxidation. *J. Lipid Res.* **30:** 885–891.
56. Keidar, S., M. Kaplan, M. Rosenblat, G. J. Brook, and M. Aviram. 1992. Apolipoprotein E and lipoprotein lipase reduce macrophage degradation of oxidized very-low-density lipoprotein (VLDL), but increase cellular degradation of native VLDL. *Metabolism.* **41:** 1185–1192.
57. Phillips, C. I., S. Tsukahara, and S. M. Gore. 1990. Corneal arcus: some morphology and applied pathophysiology. *Jpn. J. Ophthalmol.* **34:** 442–449.
58. Nordestgaard, B. G., R. Wootton, and B. Lewis. 1995. Selective retention of VLDL, IDL, and LDL in the arterial intima of genetically hyperlipidemic rabbits in vivo. Molecular size as a determinant of fractional loss from the intima-inner media. *Arterioscler. Thromb. Vasc. Biol.* **15:** 534–542.
59. Paananen, K., J. Saarinen, A. Annila, and P. T. Kovanen. 1995. Proteolysis and fusion of low density lipoprotein particles strengthen their binding to human aortic proteoglycans. *J. Biol. Chem.* **270:** 12257–12262.
60. Wissler, R. W. 1991. Update on the pathogenesis of atherosclerosis. *Am. J. Med.* **91(1B):** 3S–9S.